ADAPTIVE SUPER TWISTING DISTURBANCE OBSERVER BASED ROBUST SPEED CONTROL FOR PI-BASED FIELD ORIENTED INDUCTION MOTOR DRIVES

NGUYEN PHU DIEP, NGUYEN VAN QUOC, PHAM THUY NGOC*
Faculty of Electrical Engineering Technology, Industrial University of Ho Chi Minh City, Ho Chi Minh City, Vietnam,
** Corresponding author: phamthuyngoc@iuh.edu.vn*
DOIs: https://www.doi.org/ 10.46242/jstiuh.v83i5. 6184

Abstract. This paper proposes an adaptive super-twisting disturbance-observer-based robust speed control strategy for proportional–integral (PI)-based field-oriented control (FOC) induction motor drives. Although PI regulators are widely used in industrial FOC systems because of their simple structure, low computational burden, and practical reliability, the outer speed loop remains sensitive to load disturbances, parameter variations, and unmodeled dynamics, resulting in degraded transient performance and limited robustness. To address these limitations while preserving the conventional industrial FOC architecture, an adaptive super-twisting disturbance observer is incorporated into the speed loop, whereas standard PI controllers are retained for current and flux regulation. In that, an ASTDO observer is designed to reconstruct the lumped disturbances affecting the mechanical dynamics and generate a compensation term for the speed control loop. Through an adaptive super-twisting mechanism, the observer gains are adjusted according to the disturbance estimation error, enabling the control system to respond effectively to load torque variations and parameter uncertainties without requiring prior knowledge of disturbance bounds. The proposed PI–ASTDO structure therefore provides an adaptive and robust control mechanism while retaining the conventional FOC architecture and PI-based current and flux regulation. Lyapunov analysis is employed to establish the stability and finite-time convergence of the proposed observer. Furthermore, a hybrid genetic algorithm–particle swarm optimization (GA–PSO) method is applied to determine suitable controller parameters and further improve the dynamic characteristics of the drive. The effectiveness of the proposed structure is evaluated under rated-load operation, load torque disturbances, and rotor resistance variations. The results demonstrate improved speed-tracking performance, reduced overshoot and undershoot, smoother torque response, and enhanced disturbance rejection compared with conventional PI-based FOC and PI–STADOb control. The proposed approach also maintains low computational complexity and the practical implementation advantages of conventional industrial induction motor drives.

Keywords. Induction motor drives, Field-oriented control, Super-twisting control, Disturbance observer, Robust speed control

1 INTRODUCTION

Induction motors (IMs) remain the dominant electrical machines in industrial drive systems because of their rugged structure, low cost, high reliability, and ease of maintenance [1]–[2]. Among various control strategies, field-oriented control (FOC) has become the standard high-performance control method for IM drives because it enables decoupled torque and flux regulation with dynamic characteristics comparable to separately excited DC motors [3]–[4]. In practical FOC implementations, proportional–integral (PI) controllers are still widely employed in the speed and current loops owing to their simple structure, low computational burden, and straightforward digital implementation [5]–[6]. Consequently, PI-based FOC architectures continue to dominate commercial induction motor drive applications.

Despite these advantages, conventional PI speed controllers exhibit limited robustness under practical operating conditions. Their performance deteriorates significantly in the presence of load torque disturbances, parameter uncertainties, and unmodeled nonlinear dynamics [7]–[9]. In particular, fixed-gain PI regulators tuned under nominal conditions often produce large overshoot, slow disturbance recovery, and degraded tracking accuracy during abrupt load changes and low-speed operation [10]-[11]. These limitations become increasingly critical in modern drive applications requiring fast transient response and robust operation over a wide operating range.

To improve the performance of PI-based drive systems, numerous intelligent and adaptive tuning

© 2026 Industrial University of Ho Chi Minh City

approaches have been investigated, including fuzzy logic, neural networks, reinforcement learning, and evolutionary optimization methods [12]–[21]. Although these techniques can improve adaptability and transient performance, they generally increase controller complexity and require extensive training, heuristic tuning procedures, or high computational resources. Moreover, many intelligent tuning approaches lack rigorous stability guarantees, which limits their practical applicability in real-time motor drive systems.

Sliding mode control (SMC) has attracted considerable attention as a robust nonlinear control approach because of its inherent insensitivity to matched disturbances and parameter variations [22]–[26]. Compared with classical first-order SMC, higher-order sliding-mode techniques, particularly the super-twisting algorithm (STA), achieve finite-time convergence while significantly reducing chattering effects [27]–[31]. Consequently, STA-based controllers have been widely applied to electric drive systems to improve disturbance rejection capability and transient robustness [32]-[33]. However, most existing STA-based IM drive controllers replace the conventional PI structure entirely, resulting in increased implementation complexity and limited compatibility with existing FOC platforms.

To preserve the simplicity of PI-based FOC systems while improving robustness, several hybrid PI–SMC and PI–STA approaches have been reported [34]–[36]. Nevertheless, important limitations still remain. Most existing hybrid strategies employ fixed-gain STA structures whose performance strongly depends on gain selection and prior knowledge of disturbance bounds. In addition, excessive switching activity may increase oscillatory behavior and current ripple under varying operating conditions. These issues restrict the robustness and practical implementation capability of existing hybrid STA-based drive systems.

Motivated by these challenges, this paper proposes an adaptive super-twisting disturbance-observer-based robust speed control strategy for PI-based FOC induction motor drives. Unlike fully nonlinear drive controllers, the proposed method preserves the standard PI regulators in the current and flux loops while incorporating an adaptive super-twisting disturbance observer only in the outer speed loop. Therefore, the original FOC structure is maintained, whereas robustness against load disturbances and parameter uncertainties is significantly enhanced.

A nonlinear sliding manifold together with adaptive super-twisting gains is designed to improve convergence behavior and disturbance rejection capability without requiring prior knowledge of disturbance bounds. Furthermore, a hybrid genetic algorithm–particle swarm optimization (GA–PSO) approach is employed to optimize the key controller parameters offline, thereby improving transient performance and reducing manual tuning effort. Lyapunov-based analysis is performed to guarantee finite-time stability and boundedness of the closed-loop system.

Comparative studies under speed reversals, load torque disturbances, and stochastic perturbations demonstrate that the proposed controller achieves faster convergence, reduced overshoot, smoother torque response, and stronger robustness compared with conventional PI and fixed-gain PI–STA strategies, while maintaining low implementation complexity and practical feasibility for real-time induction motor drive applications. The main contributions of this paper are summarized as follows:

(1) An adaptive super-twisting disturbance-observer-based robust speed control strategy is developed for PI-based FOC induction motor drives while preserving the conventional PI current and flux control structure.

(2) An adaptive super-twisting disturbance observer combined with a nonlinear sliding manifold is designed to improve disturbance rejection capability and robustness against load variations, parameter uncertainties, and unmodeled dynamics.

(3) A hybrid GA–PSO optimization method is employed to determine suitable controller parameters and improve transient performance under varying operating conditions.

(4) Comparative studies demonstrate that the proposed method achieves reduced overshoot, faster disturbance recovery, smoother torque response, and improved robustness compared with conventional PI and fixed-gain PI–STA-DOb control methods while maintaining low implementation complexity.

The remainder of this paper is organized as follows. Section 2 presents the mathematical model of the induction motor and the proposed adaptive super-twisting disturbance-observer-based control strategy,

including the GA–PSO parameter optimization procedure. Section 3 presents the simulation results and discussion. Finally, Section 4 concludes the paper.

2 METHODS

2.1 Mathematical model of IMDs

In this section, the dynamic model of the induction motor is formulated in the synchronous rotating reference frame, which enables decoupled flux and torque control and forms the basis of field-oriented control (FOC). The state-space model representation can be mathematically written as the following equation:

$$\dot{x}(t)=\mathrm{A}x(t)+Bu(t) \tag{1}$$

Where: x, A, B and u can be defined as:

$$x(t)=\begin{bmatrix} i_{s\alpha} & i_{s\beta} & \varphi_{r\alpha} & \varphi_{r\beta} & \omega_r \end{bmatrix}^T;\quad u(t)=\begin{bmatrix} u_{s\alpha} & u_{s\beta} & T_L \end{bmatrix}^T$$

$$A=\begin{bmatrix} a_{11} & 0 & a_{13} & a_{14} & a_{15} \\ 0 & a_{11} & -a_{14} & a_{13} & a_{25} \\ L_m/\tau_r & 0 & -1/\tau_r & \omega_r & \varphi_{r\beta} \\ 0 & L_m/\tau_r & -\omega_r & -1/\tau_r & -\varphi_{r\alpha} \\ -b\varphi_{r\beta} & b\varphi_{r\alpha} & bi_{s\beta} & -bi_{s\alpha} & (-B/J) \end{bmatrix};\quad B=\begin{bmatrix} 1/\sigma L_s & 0 & 0 \\ 0 & 1/\sigma L_s & 0 \\ 0 & 0 & 0 \\ 0 & 0 & 0 \\ 0 & 0 & -1/J \end{bmatrix}$$

With:

$$\tau_r=\frac{L_r}{R_r};\ \sigma=1-\frac{L_m^2}{L_rL_s};\ \gamma=\frac{L_m}{L_r};\ k=\frac{3pL_m}{2L_r};\ b=\frac{k}{J}$$

$$a_{11}=-\frac{1}{\sigma L_s}\left(R_s+\frac{L_m^2}{L_r\tau_r}\right);\ a_{13}=\frac{\gamma}{\sigma L_s\tau_r};\ \mathrm{a}_{14}=-\frac{\gamma}{\sigma L_s}\omega_r;\ a_{15}=-\frac{\gamma}{\sigma L_s}\varphi_{r\beta};\ a_{25}=\frac{\gamma}{\sigma L_s}\varphi_{r\alpha}$$

The stator flux can be estimated such as:

$$\varphi_{s\alpha}=\int_0^t\left(u_{s\alpha}-R_si_{s\alpha}\right)dt;\quad \varphi_{s\beta}=\int_0^t\left(u_{s\beta}-R_si_{s\beta}\right)dt \tag{2}$$

The stator and rotor flux linkage phase is given by:

$$\varphi_s=\sqrt{\varphi_{s\alpha}^2+\varphi_{s\beta}^2};\quad \varphi_r\approx\frac{L_m}{L_r}\varphi_s \tag{3}$$

The electromagnetic torque of the induction motor can be written as:

$$T_e=\frac{3}{2}p\frac{L_m}{L_r}\varphi_ri_{sq} \tag{4}$$

The mechanical dynamics of the induction motor are governed by:

$$J\frac{d\omega_r}{dt}=T_e-T_L-B\omega_r \tag{5}$$

2.2 Adaptive Super-Twisting Disturbance-Observer-Based Speed Controller Design.

The conventional PI-based FOC offers simple implementation and satisfactory steady-state performance but remains sensitive to load disturbances, parameter uncertainties, and unmodeled mechanical dynamics, particularly under rapid operating variations. To enhance disturbance rejection while retaining the conventional PI structure, an adaptive super-twisting disturbance observer (ASTA-DOb) is incorporated into the speed loop. The resulting scheme combines the simplicity of PI regulation with the robustness and finite-time convergence of the super-twisting algorithm. The induction-motor mechanical dynamics are expressed as:

$$\dot{\omega}_r=f\left(\omega_r,i_{sq}\right)+d\left(t\right) \tag{6}$$

where $f\left(\omega_r,i_{sq}\right)$ denotes the nominal dynamics and $d\left(t\right)$ represents the lumped disturbance term including load torque variations, friction uncertainty, and parameter perturbations.

The speed tracking error is defined as:

$$e(t) = \omega_r^*(t) - \omega_r(t) \tag{7}$$

To improve convergence characteristics and suppress oscillatory behavior, the following sliding manifold is selected:

$$s(t) = \dot{e}(t) + \lambda e(t) \tag{8}$$

where λ is a positive design coefficient.

Differentiating (8) and using (6), the sliding dynamics can be expressed as:

$$\dot{s}(t) = \Psi(t) + d(t) + u_{ASTA}(t) \tag{9}$$

where $\Psi(t)$ denotes the known bounded nominal dynamics and $u_{ASTA}(t)$ is the adaptive super-twisting compensation term.

Unlike model-based linear disturbance observers, the proposed ASTA-DOb reconstructs the lumped disturbance directly from the sliding dynamics without requiring exact knowledge of disturbance bounds or accurate system parameters. The adaptive super-twisting compensation law is designed as

$$u_{STA}(t) = -\alpha(t)|s|^{1/2}\, sat(s) + z(t) \tag{10}$$

with the observer dynamics

$$\dot{z}(t) = -\beta sat(s); \quad with\ \beta > 0 \tag{11}$$

where $z(t)$ is the internal disturbance reconstruction state. The adaptive gains are updated according to:

$$\alpha = \frac{1}{2} sat(|s_\omega|) + \frac{3}{2} k_1 |s_\omega|^{1/2}\, sat(|s_\omega|) + k_1^2 |s_\omega|; \quad k_1 > 0 \tag{12}$$

where $\alpha(t)$ denotes the adaptive super-twisting gain updated online according to Eq.(12), while β is selected as a positive constant. The saturation function is defined as:

$$sat(s_\omega) = \begin{cases} 1 & if\ s_\omega > 1 \\ s_\omega & if\ |s_\omega| \le 1 \\ -1 & if\ s_\omega < -1 \end{cases}$$

Compared with fixed-gain super-twisting schemes, the adaptive mechanism increases observer gains under large errors while reducing unnecessary control action near the sliding manifold, thereby enhancing disturbance rejection and mitigating chattering.

To satisfy the super-twisting stability conditions, the adaptive gain $\alpha(t)$ is maintained strictly positive throughout the control process, while β is selected as a positive constant. When the tracking error increases due to external disturbances, the adaptive law automatically increases $\alpha(t)$, thereby providing sufficient corrective action to preserve the finite-time convergence property of the observer. As the tracking error decreases, the leakage term limits excessive gain growth, resulting in bounded adaptive gains and reduced chattering without requiring prior knowledge of the disturbance bound.

The conventional PI speed regulator is retained as

$$i_{sq}^{PI} = K_p e(t) + K_i \int e(t)\, dt \tag{13}$$

Since the q-axis current directly regulates torque under rotor-flux-oriented control, the ASTA-DOb output is converted into an equivalent current compensation term through the speed-loop input gain and added to the PI-generated reference. The resulting total q-axis current reference is given by:

$$i_{sq}^{*} = i_{sq}^{PI} + u_{STA}(t) \tag{14}$$

Hence, the proposed controller improves robustness without altering the conventional PI-based FOC structure. Define the disturbance reconstruction error as:

$$e_d(t) = z(t) - d(t) \tag{15}$$

Substituting (10) into (9) yields

$$\dot{s}(t) = -\alpha(t)|s|^{1/2}\, sat(s) + z(t) - d(t) \tag{16}$$

Using (16), (17) becomes

$$\dot{s}(t) = -\alpha(t)|s|^{1/2}\, sat(s) + e_d(t) \tag{17}$$

Taking the derivative of (15) and using (11) gives

$$\dot{e}_d(t) = -\beta sat(s) - \dot{d}(t) \tag{18}$$

Assume that the lumped disturbance and its derivative are bounded, i.e., there exist positive constants d_{max} and L such that

$$|d(t)| \le d_{max}; \quad |\dot{d}(t)| \le L; \tag{19}$$

It should be noted that the exact values of the disturbance bounds are not required in the proposed ASTA-DOB. The adaptive gain mechanism automatically adjusts the observer gains according to the tracking condition, thereby avoiding conservative gain selection based on prior knowledge of disturbance bounds. In the presence of temporary disturbance peaks beyond the assumed bounds, the observer maintains bounded operation and restores finite-time convergence once the disturbances return to the bounded region. The closed-loop system described by (17) and (18) corresponds to the canonical super-twisting structure and belongs to the class of homogeneous nonlinear systems with negative homogeneity degree. According to finite-time stability results for second-order sliding-mode systems, finite-time convergence of both $s(t)$ and $e_d(t)$ is guaranteed provided that the adaptive gains satisfy the standard super-twisting convergence conditions. Therefore, there exists a finite time $T > 0$ such that

$$s(t) \to 0; \quad e_d(t) \to 0 \tag{20}$$

for all $t \ge T$.

Furthermore, based on the strict Lyapunov construction of the super-twisting algorithm, there exists a positive-definite Lyapunov function $V(s_\omega, e_d)$ satisfying

$$\dot{V} \le -\eta V^{1/2} \tag{21}$$

where $\eta > 0$. Hence, the closed-loop system is finite-time stable in the Lyapunov sense.

Consequently, the disturbance reconstruction converges asymptotically as

$$z(t) \to d(t) \tag{22}$$

Therefore, under the proposed adaptive gain law and gain conditions, the disturbance estimation error converges in finite time, while all adaptive variables remain bounded. Hence, the proposed ASTDOb ensures robust disturbance estimation and closed-loop stability under bounded disturbances.

2.3 Offline Parameter Optimization Using GA–PSO.

The proposed adaptive super-twisting scheme requires tuning of the PI gains (K_p, K_i), super-twisting gain (k_1), and observer gain (β). To avoid time-consuming manual tuning and improve performance under nonlinear operating conditions, a hybrid genetic algorithm–particle swarm optimization (GA–PSO) framework is adopted for offline parameter optimization.

The optimization objective is formulated using the following multi-objective cost function:

$$J = w_1 \int_o^T e^2(t)dt + w_2 \int_0^T |e(t)|dt + w_3 M_p + w_4 \delta_s \tag{23}$$

where $e(t)$ is the speed tracking error, M_p denotes the overshoot, δ_s represents the settling time, and $w_i > 0$ are positive weighting coefficients used to balance the dynamic performance objectives.

The hybrid GA–PSO framework combines the complementary strengths of GA and PSO. GA provides global exploration and population diversity, mitigating premature convergence, while PSO refines promising candidates through local search to accelerate convergence. The standard PSO velocity and position updates are given by:

$$\upsilon_i^{k+1} = \rho\upsilon_i^k + c_1 r_1\left(p_i - x_i^k\right) + c_2 r_2\left(g - x_i^k\right); \quad x_i^{k+1} = x_i^k + \upsilon_i^{k+1} \tag{24}$$

where ρ is the inertia weight, c_1; c_2 are cognitive and social learning coefficients, and p_i and g denote the personal and global best solutions. Constriction factors and velocity clamping were applied to ensure stability and convergence. The swarm optimization algorithm is implemented as shown in Fig. 1.

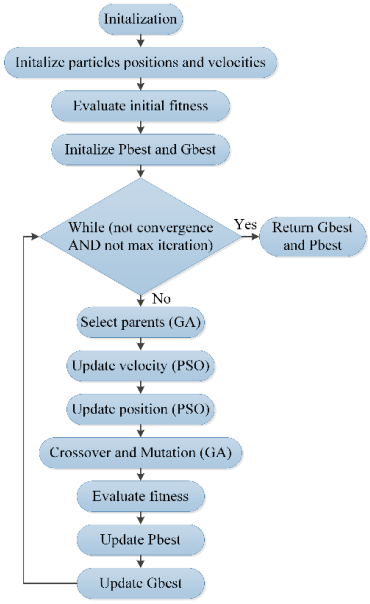


Figure 1: GA-PSO Algorithm Flowchart

Velocity clamping and convergence constraints are employed to improve optimization stability and prevent premature convergence. The optimization terminates when the maximum iteration number is reached or the improvement between consecutive iterations falls below a predefined threshold. The optimized parameters initialize the adaptive super-twisting robust compensation controller. The GA–PSO settings and optimized parameters are listed in Table 1 and kept unchanged for all simulations in Section 3, including rated-load, load-disturbance, and rotor-resistance-variation tests. Thus, the performance improvements are obtained without condition-specific retuning.

Table 1: The parameters optimization

Parameter	nPop	MaxIter	w_max	w_min	c_1	c_2	K_p	K_i	k_1	β
Value	10	20	0.9	0.5	1.5	3	35	22	1.2	0.5

The optimization converged within 20 iterations. The resulting parameters in Table I were fixed throughout all comparative simulations to ensure a fair comparison among the PI, PI-STADOb, and proposed PI-ASTDOb controllers.

3 RESULT AND DISCUSSION

The proposed adaptive super-twisting disturbance-observer-based control strategy (PI-ASTDOb) was validated through MATLAB/Simulink R2023b simulations using a 2.2-kW squirrel-cage induction motor with a rated speed of 2880 rpm. The motor parameters are: stator resistance $R_s = 1.97\ \Omega$, rotor resistance $R_r = 1.96\ \Omega$, stator inductance $L_s = 0.3739$ H, rotor inductance $L_r = 0.3739$ H, mutual inductance $L_m = 0.3585$ H, moment of inertia $J = 0.00242\ \text{kg} \cdot \text{m}^2$, and one pole pair ($p = 1$). The complete simulation model is shown in Fig. 2. All simulations were performed with a 530V DC-link voltage, a 10-kHz PWM switching frequency, a controller sampling period of 10 μs ($T_s = 1 \times 10^{-5}$ s), and the fixed-step fourth-order Runge–Kutta numerical solver. The rated electromagnetic torque is 7 N·m. The detailed speed-reference profiles, load-disturbance conditions, and rotor-resistance variation adopted in each test scenario are described in the corresponding subsections of Section 3.

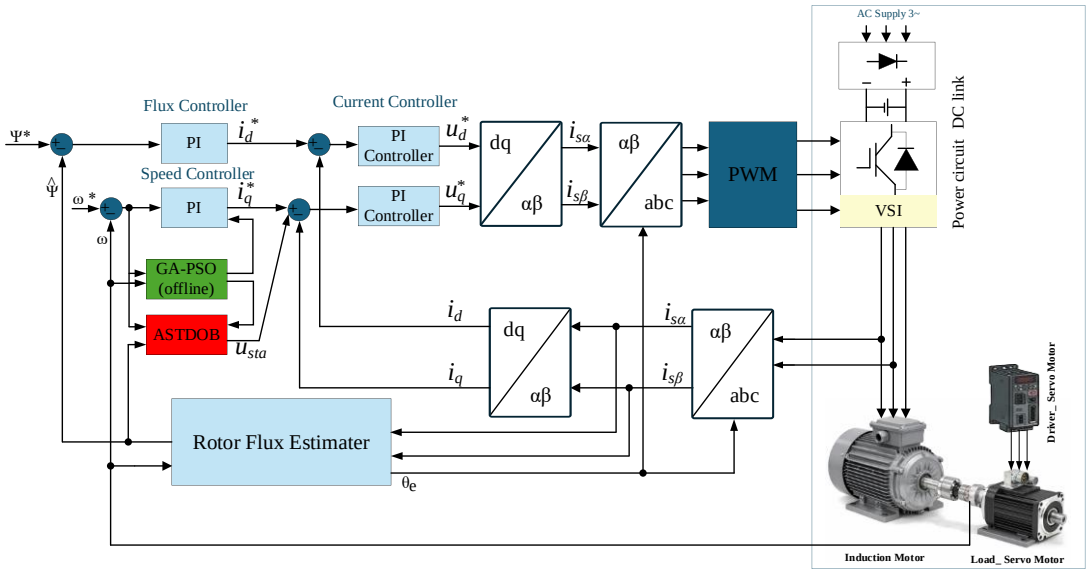


Figure 2: Overall block diagram of the proposed PI-ASTDOb-FOC induction motor drive system.

3.1 Dynamic Performance Evaluation under Rated Load Torque

Figure 3 presents the dynamic performance comparison of the conventional PI controller, the PI-STADOb controller, and the proposed PI-ASTDOb strategy under rated-load operating conditions. The reference speed profile includes multiple operating transitions to evaluate the transient response, tracking capability, and robustness of the control schemes under severe speed variations.

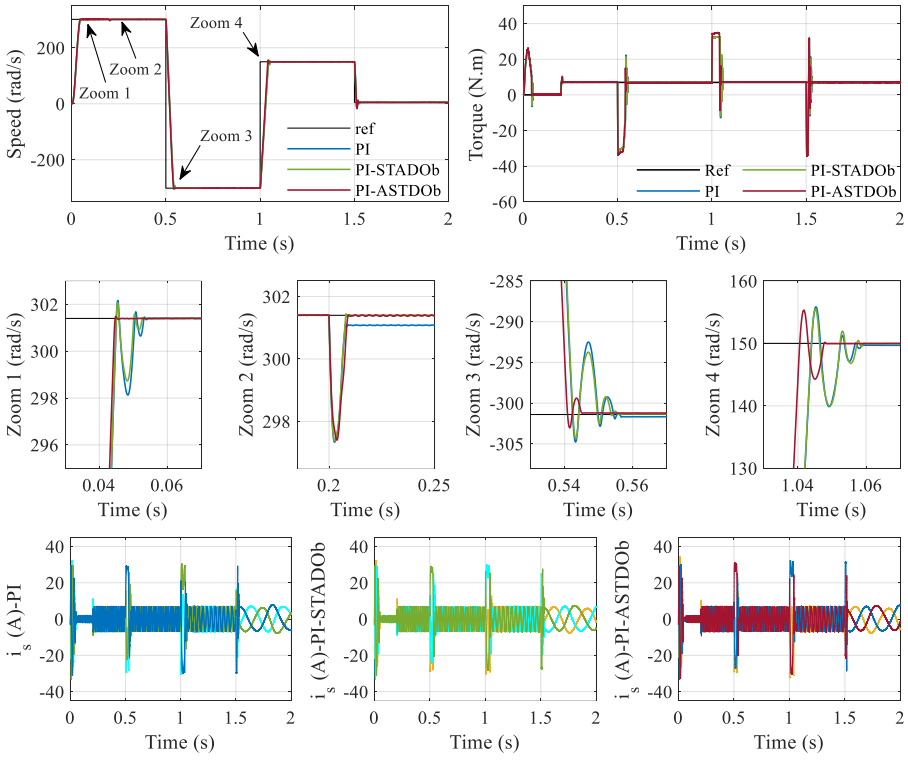


Figure 3: Dynamic performance comparison under rated load torque conditions for PI, PI-STADOb, and proposed PI-ASTDOb controllers.

The conventional PI controller exhibits relatively large overshoot and oscillatory behavior during both acceleration and deceleration transients. As observed in Zoom 1 and Zoom 4, noticeable overshoot and

undershoot appear during speed transitions due to the limited disturbance rejection capability and fixed-gain structure of the PI regulator. Furthermore, the torque response of the PI controller contains larger transient fluctuations, which lead to increased oscillations in the stator current waveforms.

The PI-STADOb controller improves the transient response compared with the conventional PI method by incorporating the super-twisting disturbance compensation mechanism. The overshoot magnitude and speed oscillations are reduced, and the torque response becomes smoother during abrupt operating transitions. However, residual oscillations are still observed near the steady-state operating points, particularly during rapid deceleration intervals shown in Zoom 3.

In contrast, the proposed PI-ASTDOb strategy achieves the best overall dynamic performance. The speed response exhibits significantly reduced overshoot and faster convergence under all operating transitions. The adaptive super-twisting disturbance observer effectively compensates for lumped disturbances and parameter uncertainties while automatically adjusting the observer gains according to the tracking condition. Consequently, the proposed controller suppresses oscillatory behavior more effectively than both the conventional PI and fixed-gain PI-STADOb approaches.

The quantitative performance comparison summarized in Table 2 further confirms the superiority of the proposed strategy. The overshoot is reduced from 0.2524% in the conventional PI controller to 0.0287% with the proposed PI-ASTDOb approach. In addition, the proposed controller achieves the lowest ISE, IAE, and RMSE values among all tested methods, indicating improved tracking accuracy and enhanced transient robustness. Although the settling-time improvement is relatively moderate, the proposed method substantially improves damping characteristics and disturbance attenuation capability without increasing the structural complexity of the conventional PI-based FOC architecture.

Table 2: Quantitative Dynamic Performance Comparison under Rated Load Torque

Control strategy	SettlingTime (s)	Overshoot (%)	ISE ($rad^2/s^2 \cdot s$)	IAE (rad/s·s)	RMSE_speed (rad/s)
PI Control	0.0437	0.2524	0.0250	0.0791	0.3163
PI-STADOb	0.0437	0.2242	0.00036	0.0025	0.0120
PI-ASTDOb	0.0431	0.0287	0.00012	0.0015	0.0068

The stator current responses also demonstrate smoother transient behavior under the proposed controller. Compared with the conventional PI and PI-STADOb methods, the proposed PI-ASTDOb strategy reduces current oscillations during abrupt speed reversals while maintaining stable steady-state current regulation. These results confirm that the proposed adaptive disturbance-observer-based compensation strategy effectively enhances the dynamic performance and robustness of PI-based induction motor drives under rated-load operating conditions.

3.2 Robustness Evaluation under Load Disturbance

Figure 4 evaluates the robustness of the PI, PI-STADOb, and proposed PI-ASTDOb controllers under abrupt load torque disturbances. The imposed load variations generate severe transient perturbations, thereby providing a stringent test of disturbance rejection capability and closed-loop stability.

The conventional PI controller exhibits clear speed deviations and oscillatory recovery during disturbance transitions. Because the PI regulator relies on fixed gains and does not explicitly compensate for external disturbances, abrupt load changes directly degrade the speed-tracking performance. This limitation is particularly evident during load application and removal intervals, where noticeable undershoot and prolonged recovery dynamics are observed.

The PI-STADOb controller improves transient robustness by introducing super-twisting disturbance compensation into the speed loop. The disturbance-induced speed deviation is reduced, and the recovery process becomes faster than that of the conventional PI controller. However, residual oscillations remain visible during repeated disturbance transitions, indicating that the fixed-gain super-twisting mechanism cannot fully adapt to varying disturbance magnitudes and operating conditions.

In contrast, the proposed PI-ASTDOb strategy achieves the most stable dynamic behavior under all

disturbance scenarios. The speed response remains tightly regulated around the reference trajectory with minimal transient deviation. This improvement is primarily attributed to the adaptive super-twisting disturbance observer, which reconstructs the lumped disturbance in finite time while automatically adjusting the observer gains according to the instantaneous tracking condition. Consequently, disturbance compensation remains effective under varying operating conditions without requiring prior knowledge of disturbance bounds.

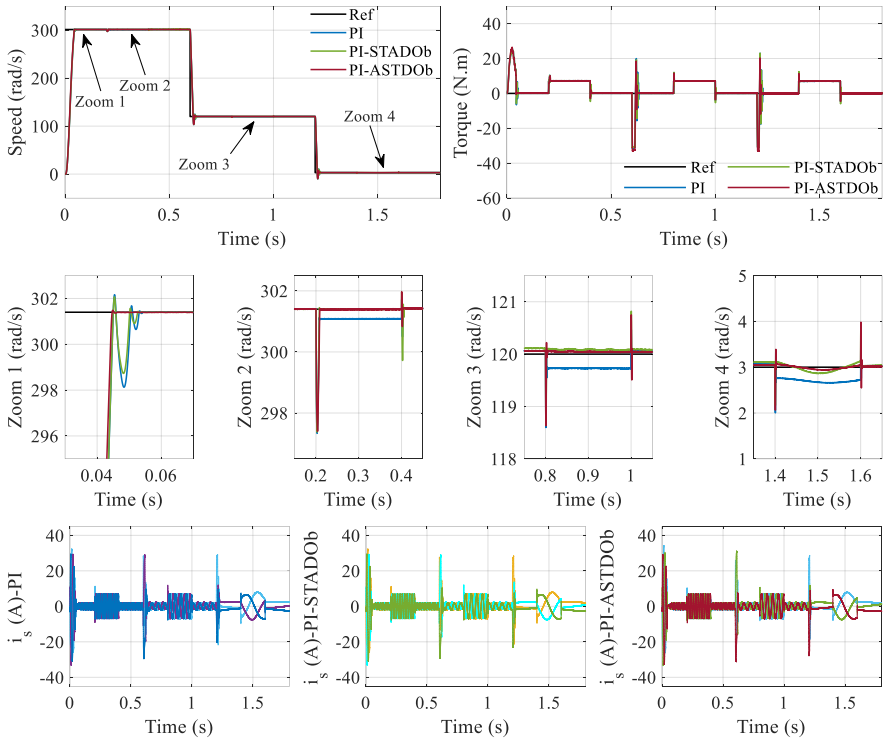


Figure 4: Comparative robustness performance under load disturbance conditions for PI, PI-STADOb, and proposed PI-ASTDOb controllers.

The electromagnetic torque response further confirms the enhanced robustness of the proposed method. Compared with PI and PI-STADOb, the proposed controller achieves smoother torque transitions and reduced oscillations during disturbance rejection. Although the super-twisting mechanism introduces high-frequency corrective action, the adaptive gain structure suppresses excessive switching near steady state, thereby improving damping and limiting oscillation propagation to the stator currents.

The stator current responses further demonstrate improved closed-loop regulation. Compared with the conventional PI controller, the proposed PI-ASTDOb maintains more stable current trajectories with reduced transient oscillations following disturbance injection. These results confirm that the proposed adaptive disturbance-observer-based compensation enhances disturbance rejection and closed-loop robustness while retaining the low-complexity structure of conventional PI-based FOC drives.

3.3 Robustness Evaluation under Rotor Resistance Variation

Figure 5 evaluates the robustness of the PI, PI-STADOb, and proposed PI-ASTDOb controllers under a 100% rotor resistance variation, where the rotor resistance is increased from its nominal value to (Rr = 2Rr nominal). Since rotor resistance directly affects rotor flux estimation and slip calculation in field-oriented control (FOC) systems, this parameter mismatch introduces flux detuning, degrades the field-orientation accuracy, and influences the transient response. Therefore, this test is conducted to evaluate the robustness of the proposed controller against severe rotor-parameter uncertainty.

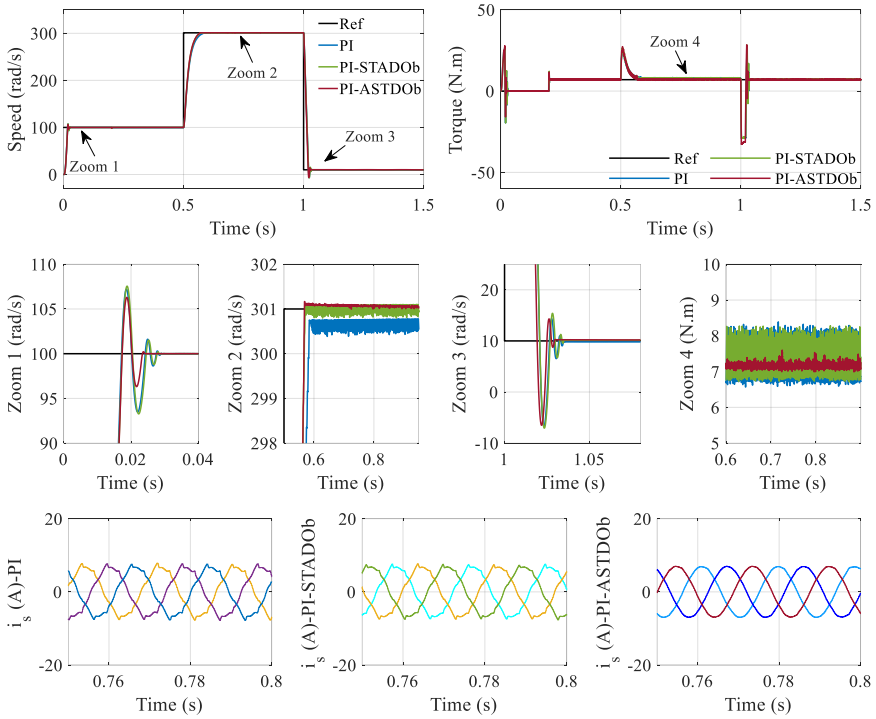


Figure 5: Comparative robustness performance under rotor resistance variation for PI, PI-STADOb, and proposed PI-ASTDOb controllers.

The conventional PI controller exhibits the highest sensitivity to rotor resistance variation. As shown in Zoom 1 and Zoom 3, pronounced overshoot, undershoot, and oscillations occur during acceleration and deceleration, while Zoom 2 reveals steady-state fluctuations and tracking deviation due to degraded field orientation under parameter mismatch. The PI-STADOb controller reduces transient oscillations and accelerates recovery through super-twisting compensation; however, residual oscillations remain due to its fixed-gain structure. In contrast, the proposed PI-ASTDOb achieves the most stable response, with significantly reduced overshoot, oscillation, and steady-state tracking error. This improvement demonstrates the effectiveness of adaptive disturbance compensation in mitigating rotor resistance mismatch while preserving closed-loop stability.

The electromagnetic torque response further confirms the enhanced robustness of the proposed controller. As shown in Zoom 4, PI-ASTDOb provides smoother torque evolution with lower oscillatory amplitude under parameter variation. Its adaptive gain mechanism enables stronger compensation during transients while reducing unnecessary corrective action near steady state, thereby attenuating torque ripple propagation.

The stator currents provide further evidence of improved regulation. Under rotor resistance mismatch, the conventional PI controller exhibits pronounced current oscillations and waveform distortion, indicating degraded decoupling and regulation performance. PI-STADOb partially improves current stability but retains residual ripple, whereas PI-ASTDOb maintains smoother and more balanced three-phase currents with reduced oscillatory propagation. Overall, the proposed strategy enhances robustness to rotor resistance variation, yielding improved speed tracking, smoother torque response, and better current regulation while retaining the low-complexity structure of conventional PI-based FOC.

4 CONCLUSIONS

This paper has presented an adaptive super-twisting disturbance-observer-based robust speed control strategy for PI-based field-oriented induction motor drives. The proposed approach preserves the conventional PI–FOC structure while enhancing robustness through an adaptive super-twisting disturbance compensation mechanism integrated into the outer speed loop. A nonlinear sliding manifold together with

adaptive super-twisting gains was designed to improve convergence behavior and disturbance rejection capability without requiring prior knowledge of disturbance bounds. Lyapunov-based analysis confirmed finite-time stability and boundedness of the closed-loop system.

Simulation results under rated-load operation, load torque disturbances, and rotor resistance variation demonstrated that the proposed PI-ASTDOb strategy achieves reduced overshoot, faster disturbance recovery, smoother torque response, and improved robustness compared with conventional PI and fixed-gain PI-STADOb controllers. In addition, the proposed method maintained more stable stator current regulation and reduced oscillatory propagation under parameter uncertainty and disturbance conditions. These improvements were achieved without increasing the structural complexity of the conventional PI-based FOC architecture, thereby preserving practical feasibility for industrial induction motor drive applications.

Future work will focus on the real-time implementation of the proposed PI-ASTDOb strategy on a DSP-based induction motor drive platform. Particular attention will be devoted to experimentally evaluating stator current ripple and chattering characteristics under practical non-ideal conditions, including sensor measurement noise, inverter dead-time, switching delays, and PWM implementation effects. In addition, adaptive parameter estimation and sensorless flux-observer techniques will be investigated to improve robustness against wider parameter uncertainty and low-speed operating conditions. Future studies will also consider extending the proposed disturbance-observer-based framework to energy-efficient and fault-tolerant induction motor drive applications under varying load profiles and nonlinear operating environments.

REFERENCES

[1] I. Boldea and S. A. Nasar, *Electric Drives*, 3rd ed. Boca Raton, FL, USA: CRC Press, 2016.
[2] B. K. Bose, *Modern Power Electronics and AC Drives*. Upper Saddle River, NJ, USA: Prentice Hall, 2002.
[3] F. Blaschke, “The principle of field orientation as applied to the new transvector closed-loop control system for rotating-field machines,” *Siemens Review*, vol. 39, no. 5, pp. 217–220, 1972.
[4] R. Krishnan, *Electric Motor Drives: Modeling, Analysis, and Control*. Upper Saddle River, NJ, USA: Prentice Hall, 2001.
[5] W. Song, J. Li, C. Ma, Y. Xia, and B. Yu, “A simple tuning method of PI regulators in FOC for PMSM drives based on deadbeat predictive conception,” *IEEE Trans. Transp. Electrific*, vol. 10, no. 4, pp. 852–863, Dec. 2024.
[6] N. Goel, S. Chacko, and R. Patel, “PI controller tuning based on stochastic optimization technique for performance enhancement of DTC induction motor drives,” *J. Inst. Eng. (India), Series B*, vol. 101, pp. 1–8, 2020.
[7] X. Sun, Z. Su, G. Lei, and M. Yao, “Robust predictive cascaded speed and current control for PMSM drives considering parameter variations,” *IEEE Trans. Ind. Electron*, vol. 71, no. 9, pp. 10235–10245, Sep. 2024.
[8] J. Wang, F. Wang, Z. Zhang, S. Li and J. Rodríguez, "Design and Implementation of Disturbance Compensation-Based Enhanced Robust Finite Control Set Predictive Torque Control for Induction Motor Systems," in *IEEE Transactions on Industrial Informatics*, vol. 13, no. 5, pp. 2645-2656, Oct. 2017.
[9] T. Uzunović, F. G. Montoya, A. Osmanović, F. M. Arrabal-Campos, A. Alcayde, A. H. Eid, and A. Šabanović, “Combining real-time parameter identification and robust control algorithms for effective control of electrical machines,” in *Proc. Int. Conf. Electrical Machines (ICEM)*, 2022, pp. 2391–2396.
[10] A. Lokriti, I. Salhi, S. Doubabi, and Y. Zidani, “Induction motor speed drive improvement using fuzzy IP self-tuning controller: A real-time implementation,” *ISA Transactions*, vol. 52, no. 3, pp. 406–417, 2013.
[11] R. Marouane and Z. Malika, “Particle swarm optimization for tuning PI controller in FOC chain of induction motors,” in *Proc. 4th Int. Conf. Optimization and Applications (ICOA)*, pp. 1–5, 2018.
[12] R. Arulmozhiyal and K. Baskaran, “Implementation of a fuzzy PI controller for speed control of induction motors using FPGA,” *Journal of Power Electronics*, vol. 10, no. 1, pp. 65–71, 2010.
[13] H. Li, B. Song, T. Chen, Y. Xie, and X. Zhou, “Adaptive fuzzy PI controller for permanent magnet synchronous motor drive based on predictive functional control,” *J. Franklin Inst*, vol. 358, no. 15, pp. 7333–7364, 2021.
[14] W. Shipman and L. Coetzee, “Reinforcement learning and deep neural networks for PI controller tuning,” *IFAC-PapersOnLine*, vol. 52, no. 29, pp. 111–116, 2019.
[15] U. Alejandro-Sanjines, V. Asanza, L. Lorente, and D. Peluffo-Ordóñez, “Adaptive PI controller based on a reinforcement learning algorithm for speed control of a DC motor,” *Biomimetics*, vol. 8, no. 5, p. 434, 2023.

[16] I. Djelamda and I. Bouchareb, "Field-oriented control based on adaptive neuro-fuzzy inference system for PMSM dedicated to electric vehicle," *Bull. Electr. Eng. Informat*, vol. 11, no. 4, pp. 1892–1901, 2022.
[17] F. Saidi, F. Naceri, L. Youb, M. Cernat, and L. Guasch Pesquer, "Two types of fuzzy logic controllers for the speed control of the doubly-fed induction machine," *Adv. Electr. Comput. Eng*, vol. 20, no. 3, pp. 65–74, 2020.
[18] V. Kaliappan, "Nonlinear PID controller parameter optimization using enhanced genetic algorithm for nonlinear control system," *Journal of Control Engineering and Applied Informatics*, vol. 18, no. 2, pp. 3–10, 2016.
[19] Z. Chu, Q. Guo, and C. Wang, "The PID control algorithm based on whale optimization algorithm optimized BP neural network," in *Proc. IEEE 7th Information Technology and Mechatronics Engineering Conf. (ITOEC)*, pp. 2450–2453, 2023.
[20] N. Farah, M. H. N. Talib, Z. Ibrahim, N. Abd. Rahim, R. Zulhani, N. Nordin and A. M. Razali, "A novel self-tuning fuzzy logic controller based induction motor drive system: An experimental approach," *IEEE Access*, vol. 7, pp. 68172–68184, 2019.
[21] J. Prabhakaran, P. Thirumoorthi, M. Mathankumar, et al., "Development of intelligent controller for high-performance electric drives with hybrid CSA and RERNN technique," *Scientific Reports*, vol. 15, p. 14020, 2025.
[22] L. Wu, J. Liu, S. Vazquez, and S. K. Mazumder, "Sliding mode control in power converters and drives: A review," *IEEE/CAA Journal of Automatica Sinica*, vol. 9, no. 3, pp. 392–406, 2022.
[23] Y. Shtessel, C. Edwards, L. Fridman, and A. Levant, *Sliding Mode Control and Observation*. New York, NY, USA: Springer, 2014.
[24] L. Fridman, A. Poznyak, and F. J. Bejarano, *Robust Output LQ Optimal Control via Integral Sliding Modes*. Cham, Switzerland: Birkhäuser, 2014.
[25] C. A. Martínez-Fuentes, U. Pérez-Ventura, and L. Fridman, "Chattering analysis for Lipschitz continuous sliding-mode controllers," *Int. J. Robust Nonlinear Control*, vol. 31, no. 9, pp. 3779–3794, 2021.
[26] L. Qu, W. Qiao, and L. Qu, "Active-disturbance-rejection-based sliding-mode current control for permanent-magnet synchronous motors," *IEEE Transactions on Power Electronics*, vol. 36, no. 1, pp. 751–760, Jan. 2021
[27] N. T. Pham and P. D. Nguyen, "A Novel Adaptive Hybrid FZBS_STASOSM Controller for IM Drives", *J Robot Control (JRC)*, vol. 6, no. 5, pp. 2389–2398, Oct. 2025.
[28] R. Seeber and M. Reichhartinger, "Conditioned super-twisting algorithm for systems with saturated control action," *Automatica*, vol. 116, p. 108921, 2020.
[29] S. Ding, Q. Hou, and H. Wang, "Disturbance-observer-based second-order sliding mode controller for speed control of PMSM drives," *IEEE Transactions on Energy Conversion*, vol. 38, no. 1, pp. 100–110, Mar. 2023.
[30] B. Wang, T. Wang, Y. Yu, and D. Xu, "Second-order terminal sliding-mode speed controller for induction motor drives with nonlinear control gain," *IEEE Trans. Ind. Electron*, vol. 70, no. 11, pp. 10923–10934, Nov. 2023.
[31] J. H. Yi, S. You, Y. Lee, and W. Kim, "Super-twisting-based nonlinear gain sliding mode controller for position control of permanent-magnet synchronous motors," *IEEE Access*, vol. 9, pp. 155187–155198, 2021.
[32] Z. Tang, L. Wang, D. Wang, and X. Li, "Robust speed control of motor-driven servo systems via an adaptive disturbance rejection terminal sliding mode controller," *IEEE Trans. Ind. Electron*, vol. 72, no. 12, pp. 14425–14436, Dec. 2025.
[33] C. Li, T. Pan, and S. Ding, "Finite-time fast integral terminal sliding-mode speed control method with disturbance observer for SPMSM," *IEEE Transactions on Power Electronics*, vol. 40, no. 8, pp. 10694–10704, Aug. 2025.
[34] A. Nurettin and N. İnanç, "High-performance induction motor speed control using a robust hybrid controller with a supertwisting sliding mode load disturbance observer," *IEEE Trans. Ind. Electron*, vol. 70, no. 8, pp. 7743–7752, Aug. 2023.
[35] N. T. Pham and T. D. Le, "A novel FOC vector control structure using RBF tuning PI and sliding mode for SPIM drives," *International Journal of Intelligent Engineering Systems*, vol. 13, no. 5, pp. 429–440, 2020.
[36] N. T. Pham, "Design of novel STASOSM controller for FOC control of dual-star induction motor drives," *International Journal of Robotics and Control Systems*, vol. 4, no. 3, pp. 1059–1074, 2024.

ĐIỀU KHIỂN TỐC ĐỘ BỀN VỮNG DỰA TRÊN BỘ QUAN SÁT NHIỄU THÍCH NGHI TRƯỢT SIÊU XOẮN CHO ĐIỀU KHIỂN ĐỊNH HƯỚNG TRƯỜNG CHO HỆ TRUYỀN ĐỘNG ĐỘNG CƠ KHÔNG ĐỒNG BỘ BA PHA

NGUYỄN PHÚ ĐIỆP, NGUYỄN VĂN QUỐC, PHẠM THÚY NGỌC*
Khoa Công Nghệ Điện – Trường Đại học Công Nghiệp Thành Phố Hồ Chí Minh
** Tác giả liên hệ: phamthuyngoc@iuh.edu.vn*

Tóm tắt. Bài báo này đề xuất một chiến lược điều khiển thích nghi kết hợp bộ điều khiển PI với bộ quan sát nhiễu thích nghi trượt siêu xoắn (ASTDO) để thực hiện điều khiển định hướng trường (FOC) cho hệ thống truyền động động cơ không đồng bộ. Chiến lược đề xuất kết hợp các đặc tính đơn giản và tin cậy của bộ điều khiển PI truyền thống với khả năng ước lượng và bù nhiễu của bộ quan sát thích nghi trượt super-twisting, qua đó nâng cao hiệu suất điều chỉnh tốc độ và tính bền vững của hệ thống trong các điều kiện vận hành nhiễu loạn tải, biến đổi tham số và động lực học không được mô hình hóa. Bộ quan sát ASTDO được thiết kế để tái tạo các nhiễu tổng hợp tác động lên động lực học cơ khí và tạo ra thành phần bù cho vòng điều khiển tốc độ. Thông qua cơ chế thích nghi trượt siêu xoắn, các hệ số của bộ quan sát được điều chỉnh dựa trên sai số ước lượng nhiễu, cho phép hệ thống điều khiển phản ứng hiệu quả với sự thay đổi mô-men tải và sự bất định về tham số mà không cần biết trước giới hạn của nhiễu. Do đó, cấu trúc PI–ASTDO đề xuất mang lại cơ chế điều khiển thích nghi và bền vững, đồng thời vẫn duy trì kiến trúc FOC truyền thống cùng phương pháp điều chỉnh dòng điện và từ thông dựa trên bộ điều khiển PI. Phân tích Lyapunov được sử dụng để chứng minh tính ổn định và khả năng hội tụ trong thời gian hữu hạn của bộ quan sát đề xuất. Hơn nữa, phương pháp lai giữa thuật toán di truyền (GA) và tối ưu hóa bầy đàn hạt (PSO) được áp dụng để xác định các tham số bộ điều khiển phù hợp và cải thiện hơn nữa các đặc tính động học của hệ thống truyền động. Hiệu quả của cấu trúc đề xuất được đánh giá trong các điều kiện vận hành ở tải định mức, chịu nhiễu mô-men tải và thay đổi điện trở rotor. Kết quả cho thấy hiệu suất bám tốc độ được cải thiện, độ vọt lố (overshoot) và độ giảm tốc (undershoot) được giảm thiểu, đáp ứng mô-men nhanh hơn, khả năng loại bỏ nhiễu được tăng cường so với phương pháp FOC dựa trên PI truyền thống và phương pháp PI–STADO. Phương pháp đề xuất cũng duy trì độ phức tạp tính toán thấp và các ưu điểm về triển khai thực tế của các hệ thống truyền động động cơ không đồng bộ công nghiệp truyền thống.
Từ khóa: Hệ truyền động động cơ không đồng bộ, Điều khiển định hướng từ trường, Điều khiển Super-twisting, Bộ quan sát nhiễu, Điều khiển tốc độ bền vững.

Received on August 21 – 2026
Revised on October 08 – 2026